OLD DOMINION UNIVERSITY RESEARCH FOUNDATION

DEPARTMENT OF PHYSICS AND GEOPHYSICAL SCIENCES
SCHOOL OF SCIENCES AND HEALTH PROFESSIONS
OLD DOMINION UNIVERSITY
NORFOLK, VIRGINIA

Technical Report PGSTR-PH76-24

A HIGH-TEMPERATURE WIDEBAND PRESSURE TRANSDUCER

By

Allan J. Zuckerwar

Progress Report

Prepared for the
National Aeronautics and Space Administration
Langley Research Center
Hampton, Virginia

Under
Grant NSG 1039-1
September 1975 - March 1976

March 1976

DEPARTMENT OF PHYSICS AND GEOPHYSICAL SCIENCES
SCHOOL OF SCIENCES AND HEALTH PROFESSIONS
OLD DOMINION UNIVERSITY
NORFOLK, VIRGINIA

Technical Report PGSTR-PH76-24

A HIGH-TEMPERATURE WIDEBAND PRESSURE TRANSDUCER

By

Allan J. Zuckerwar

Progress Report

Prepared for the
National Aeronautics and Space Administration
Langley Research Center
Hampton, Virginia 23665

Under
Grant NSG 1039-1
September 1975 - March 1976
Harlan K. Holmes, Technical Monitor
Instrument Research Division

Submitted by the
Old Dominion University Research Foundation
Norfolk, Virginia 23508

March 1976

A HIGH TEMPERATURE WIDEBAND PRESSURE TRANSDUCER

1. INTRODUCTION

Effort during the first two quarters of NSG 1039-1 was devoted almost exclusively to the problem of operating a condenser microphone as the terminal element of a half-wavelength transmission line. The hostile environment in which the condenser microphone will be situated necessitates roughly a 25-foot separation from its supporting electronics. A theoretical analysis of the microphone-cable system, substantiated by laboratory tests on several cables, provides design criteria to optimize the system gain.

A summary of results concerning the cable problem will be presented at the 91st Meeting of the Acoustical Society of America, April 5-9, 1976, in a talk entitled "Operation of a Condenser Microphone as the Terminal Element of a Half-Wavelength Transmission Line in an AM Carrier System."

2. THEORETICAL ANALYSIS

A block diagram of the microphone system is shown in figure 1. Pressure fluctuations produce capacitance changes in the condenser microphone, which amplitude-modulate the carrier voltage provided by the carrier electronics. At the output of the latter appears a demodulated signal, proportional to the amplitude of the pressure fluctuations, and measured or recorded on an output device. A lossless cable, having a length ℓ equal to a half-wavelength of the carrier voltage (or an integral multiple thereof), would reflect the condenser microphone directly to the output terminals of the carrier electronics. However, the losses of the cable, ever present in practice, lead to a substantial reduction in system sensitivity. The goal of this phase of the investigation is to find criteria for holding the detrimental effects of the cable to a minimum.

A circuit diagram of the front end (elements connected to gate 1 of the FET) of the converter (refs. 1 and 2), is shown in figure 2a.

Elements L, C_o, and R represent the tank circuit, C the condenser microphone, and Z_S and Z_R the impedance at the sending and receiving ends of the cable, respectively. The admittance Y_T between gate 1 and common is the following:

$$Y_T = \frac{1}{j\omega L} j\ \omega\ C_o + \frac{1}{R} + \frac{1}{Z_S} \quad , \tag{1}$$

where ω is the carrier angular frequency. If the losses of the cable are small, the admittance Y_S looking into the sending end of the cable can be approximated as follows (ref. 3):

$$Y_S = \frac{1}{Z_S} = \frac{1}{R_o} \left[\frac{\alpha\ell(1 - \omega CR_o \tan \omega\tau) + j(\omega CR_o + \tan \omega\tau)}{(1 - \omega CR_o \tan \omega\tau) + j\alpha\ell(\omega CR_o + \tan \omega\tau)} \right], \tag{2}$$

where α = attenuation constant of the cable [neper/m]

τ = ℓ/c = transit time from one end of the cable to the other [sec]

c = velocity of propagation [m/sec]

R_o = characteristic impedance of the cable [Ω].

Near the resonant frequencies of the cable it will always be true that

$$|\omega CR_o \tan \omega\tau| << 1 \quad . \tag{3}$$

Using the inequality (3) and substituting equation (2) into (1), we obtain an approximate expression for Y_T near the resonant frequencies of the cable:

$$Y_T \approx j\left[-\frac{1}{\omega L} + \omega(C_o + C) + \frac{\tan \omega\tau}{R_o} \right] + \frac{1}{R} + \frac{\alpha\ell}{R_o} \left[1 + (\omega CR_o + \tan \omega\tau)^2 \right] . \tag{4}$$

Resonance occurs when the imaginary part of equation (4) vanishes:

$$-\frac{1}{\omega L} + \omega(C_o + C) + \frac{\tan \omega\tau}{R_o} = 0 \quad . \tag{5}$$

By applying Newton's Rule we obtain an approximate solution for the resonant angular frequencies ω_R:

$$\omega_R \approx \frac{n\pi}{\tau} + \frac{R_o}{n\pi L} \frac{(1 - n^2\pi^2/\omega_o^2\tau^2)}{\left[1 + (R_o/\omega_o^2 L\tau)(1 + \omega_o^2 \tau^2/n^2\pi^2)\right]} \quad , \tag{6}$$

$$(n = 1, 2, 3, \ldots) \quad ,$$

where $\omega_o = (LC_o)^{-1/2}$ = resonant angular frequency of the isolated tank circuit. Hence the coupling between the cable and the tank circuit renders the sequence of frequencies anharmonic. If both the tank circuit and the cable, in its fundamental mode, are tuned to the carrier frequency, it follows that:

$$\omega_o \tau = \pi \quad . \tag{7}$$

In practice, equation (7) is only approximately fulfilled owing to imprecision in cutting the cable and to the effect of the cable connectors. In the present application it is true that

$$R_o/\pi L << \pi/\tau \quad . \tag{8}$$

In view of expressions (7) and (8), the anharmonicity becomes greater with increasing n but remains small for the first several values of n.

It will be found convenient to represent the cable by an equivalent parallel tank circuit, as shown in figure 2b, which will be valid near the cable resonances. The last term in equation (4) represents the equivalent parallel resistance R_ℓ:

$$\frac{1}{R_\ell} = \frac{\alpha \ell}{R_o} \left[1 + (\omega C R_o + \tan \omega\tau)^2\right] \quad . \tag{9}$$

The equivalent capacitance C_ℓ and inductance L_ℓ, when isolated, must yield the cable resonances:

$$L_\ell C_\ell = \tau^2/n^2\pi^2 \quad . \tag{10}$$

Furthermore, the circuit of figure 2b must yield the resonant frequencies given by equation (6):

$$\left(\frac{LL_\ell}{L + L_\ell}\right) (C + C_o + C_\ell) = \frac{1}{\omega_R^2} \quad . \tag{11}$$

Equations (10) and (11) yield the following expressions for C_ℓ and L_ℓ:

$$C_\ell = \frac{\tau}{2R_o} \left[1 - \frac{R_o}{\omega_o^2 L\tau} \left(1 - \frac{\omega_o^2\tau^2}{n^2\pi^2}\right)\right] \quad , \tag{12a}$$

$$L_\ell = \frac{2R_o\tau}{n^2\pi^2 \left[1 - \frac{R_o}{\omega_o^2 L\tau} \left(1 - \frac{\omega_o^2\tau^2}{n^2\pi^2}\right)\right]} \quad . \tag{12b}$$

The admittance of the circuit shown in figure 2b may be written

$$Y_T = j\left[-\frac{1}{\omega}\left(\frac{1}{L} + \frac{1}{L_\ell}\right) + \omega(C + C_o + C_\ell)\right] + \frac{1}{R} + \frac{1}{R_\ell} \quad . \tag{13}$$

According to equations (12) and (18) of reference 1 the conversion gain s of the carrier electronics (output voltage per unit pressure amplitude) can be written in the form

$$s = K[Q/(C + C_o + C_\ell)]^2 \quad , \tag{14}$$

where K depends upon parameters of the electronic circuit and Q is the quality factor of the circuit of figure 2b.

$$Q = \omega_R(C + C_o + C_\ell)\left(\frac{RR_\ell}{R + R_\ell}\right) \quad . \tag{15}$$

Substituting for Q in equation (14) we find

$$s = K\left(\frac{\omega_R RR_\ell}{R + R_\ell}\right)^2 \quad . \tag{16}$$

The conversion gain without the cable is

$$s_o = K\omega_o^2 R^2 \quad . \tag{17}$$

Then the output voltage with the cable, relative to that without the cable, is given by the following expression:

$$\begin{aligned} \text{Output voltage [dB]} &= 20 \log (s/s_o) \\ &= 40 \log [\omega_R R_\ell/\omega_o(R + R_\ell)] \quad . \end{aligned} \tag{18}$$

Near the resonant frequencies we may neglect $\tan \omega\tau$ in equation (9) and then substitute the resulting approximate expression for R_ℓ into equation (18):

$$\begin{aligned} \text{Output voltage [dB]} = 40 \log \Big\{ &\omega_R R_o/\omega_o [R_o + R\alpha\ell \\ &\times (1 + \omega_R^2 C^2 R_o^2)] \Big\} \quad . \end{aligned} \tag{19}$$

Under the conditions of the present experiments $R_o << R\alpha\ell$. Thus

$$\text{Output voltage [dB]} \approx 40 \log \left[\omega_R R_o / \omega_o R \alpha \ell \times (1 + \omega_R^2 C^2 R_o^2) \right] \quad . \tag{20}$$

Equation (20) shows that a high output voltage is favored by a high value of the ratio $R_o/\alpha\ell$, i.e., high characteristic impedance and, of course, low cable losses. This ratio at some fixed frequency may be regarded as a figure of merit for the cable.

3. EXPERIMENTAL RESULTS

Examination of equation (19) reveals that we must know the equivalent parallel resistance R of the original tank circuit as well as the cable attenuation α in order to compare experimental results with theory. Both quantities are, in general, frequency dependent.

The equivalent parallel resistance R was determined by the method suggested by equation (16) of reference 1 (utilizing the difference in frequencies at the positive and negative peaks of the converter transfer function). Varying the capacitance of the varactor diodes and adding external capacitance permitted determination of R over the frequency range 8 to 14 MHz. The data fit the expression

$$R = 43754\ f^{-0.73}\ [\Omega] \quad (f \text{ in MHz}) \quad ,$$

which was used over the entire frequency range investigated (7 to 50 MHz).

The frequency dependence of the attenuation coefficient α was determined from measurements using a Hewlett-Packard Model 4815A Vector Impedance Meter. The α values were found slightly higher than those listed in reference 4, probably as a result of connector losses, but agreement was generally good. The attenuation values for all the cables tested, shown in figure 3, fit expressions of the form

$$\alpha = Df^A \quad .$$

Values of D and A, as well as the characteristic impedance R_o, length ℓ, and figure of merit at 10 MHz $R_o/\alpha_{10}\ell$ are listed in table 1. Other parameters entering equation (19) have the following values:

$$\omega_o = 65.1353 \times 10^6 \text{ radian/sec}$$

$$C = 17.7 \text{ pf} \quad .$$

A block diagram of the instrumentation used to test the system sensitivity with various cables is shown in figure 4. The microphone is excited by means of an acoustic calibrator, driven externally by the test oscillator-power amplifier combination. The test cable connects the microphone to gate 1 of the FET in the converter. The converter-zero drive system is the same as that described in references 1 and 2 except for the chassis, a conventional minibox in place of the stainless steel tube, which contains jacks for connecting the cable and an external carrier voltage to drive gate 2 of the FET. The rf signal generator provides the carrier voltage, and a digital true rms voltmeter measures the output voltage. Both the acoustical and carrier frequencies are monitored on electronic counters.

The level of acoustical excitation was adjusted for 130 dB at 1 kHz for all measurements. The rf signal generator was tuned to a resonant frequency of the coupled tank circuit-cable system, and the output voltage of the zero drive amplifier recorded; this procedure was repeated to obtain data, in most cases, for the first six resonant frequencies. A measurement was also made with the microphone connected directly to the converter in order to establish the output reference voltage (0 dB).

Figure 5 shows the theoretical [equation (19)] and experimental output voltages versus carrier frequency for the coaxial cables. Only a single adjustment factor was used to fit all the data points to the theoretical curves. Agreement between theory and experiment is generally good except for the 30Ω high-temperature cable, for which the sensitivity is underestimated. The cause of this discrepancy is

unknown. The roll-off of the experimental points beyond 31.6 MHz is attributed to the deterioration of the quality factor of the inductor. Figure 6 shows the response of a two-wire, 300Ω unshielded antenna cable. The same adjustment factor was used here as for the cables in figure 5. Agreement between theory and experiment beyond the fundamental carrier frequency is poor, owing to erratic behavior of the cable parameters within the mid-range of carrier frequencies.

The results presented in figures 5 and 6 enable us to draw the following conclusions:

a. Because the response of a cable included in figure 5 or 6 has a direct correspondence with its figure of merit, $R_o/\alpha\ell$ (see table 1), it is desirable to use a cable with the highest possible figure of merit.

b. System sensitivity, with the coaxial cables, increases with carrier frequency. It is desirable to use a higher carrier frequency than the 10 MHz in the original converter.

c. The use of a high quality cable, together with a high carrier frequency, may confine the loss of system sensitivity to within a few dB. So far, in the best case, the loss was held to about 7 dB.

d. The design of the high-temperature cable, using alumina beads and a stainless steel shield, is inadequate for the present application.

4. FUTURE WORK

a. Three approaches to the high-temperature cable problem will be considered:

(1) A composite cable, consisting of a 4-foot-high temperature section connected at one end to the microphone and at the other end to a conventional cable.*

---

* Preliminary results on such an arrangement, together with an in-house fabricated high-temperature microphone, indicate a noise floor of about 110 dB at room temperature. This system will be used for initial temperature tests.

(2) A commercially available semi-rigid hermetically sealed cable using a quartz powder dielectric. Bids have been solicited from two manufacturers.

(3) A redesigned cable, using alumina beads, copper shield, and a smaller inner conductor to increase the characteristic impedance.

b. The cable impedance, as seen from gate 1 of the FET, could possibly be increased by means of an rf transmission line transformer (ref. 5).

c. A test oven, presently under construction, will be completed and high-temperature testing initiated.

d. The microphone cartridge will be redesigned to extend its frequency response.

REFERENCES

1. A.J. Zuckerwar and W.W. Shope, IEEE Transactions Instrum. Meas., IM-23, pp. 23-27 (1974).

2. A.J. Zuckerwar, "Automatic Tuning and Remote Calibration of a Microphone Carrier System", Final Technical Report, NAS1-11707-29 (1974).

3. J.D. Ryder, Networks, Lines, and Fields, Prentice-Hall (1955), p. 340.

4. Catalog ACD-5, Amphenol Corp. Cable Division.

5. C.L. Ruthroff, Proc. IRE 47, 1337-1342 (1959).

Table 1. Cable parameters

Cable	Type	Characteristic Impedance	Attenuation Parameters		Length	Figure of Merit
		R_o	D	A	ℓ	$R_o/a_{10}\ell$
		Ω	neper/m		m	
Instrum. cable	Coaxial	76	1.66×10^{-3}	0.53	10.75	1257
Hi-temp. cable	Coaxial	30	2.83×10^{-3}	0.53	7.62	411
RG 62 A/U	Coaxial	95	1.13×10^{-3}	0.53	15.11	1642
RG 58 C/U	Coaxial	51	1.66×10^{-3}	0.53	11.10	817
RG 11 A/U	Coaxial	76	9.44×10^{-4}	0.53	11.19	2123
RG 59 B/U	Coaxial	76	1.36×10^{-3}	0.53	11.14	1480
Belden 8230	Parallel-wire	300	1.74×10^{-4}	1.48	13.43	4150

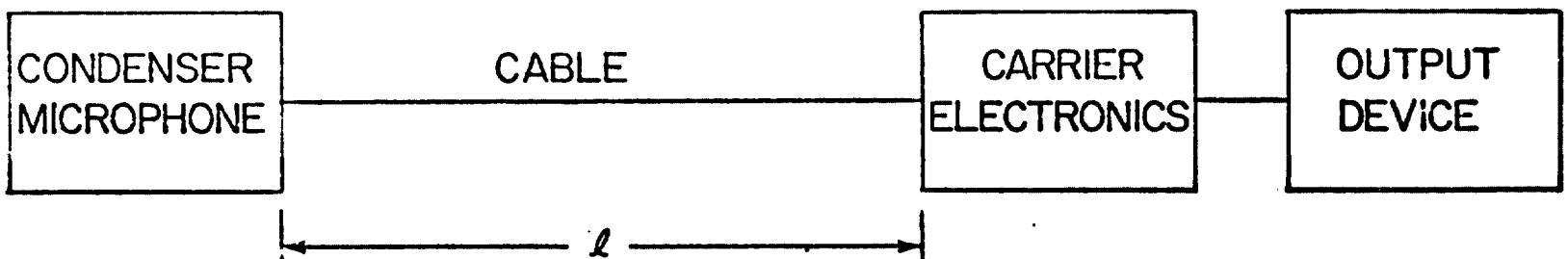

Figure 1. Block diagram of high-temperature microphone system.

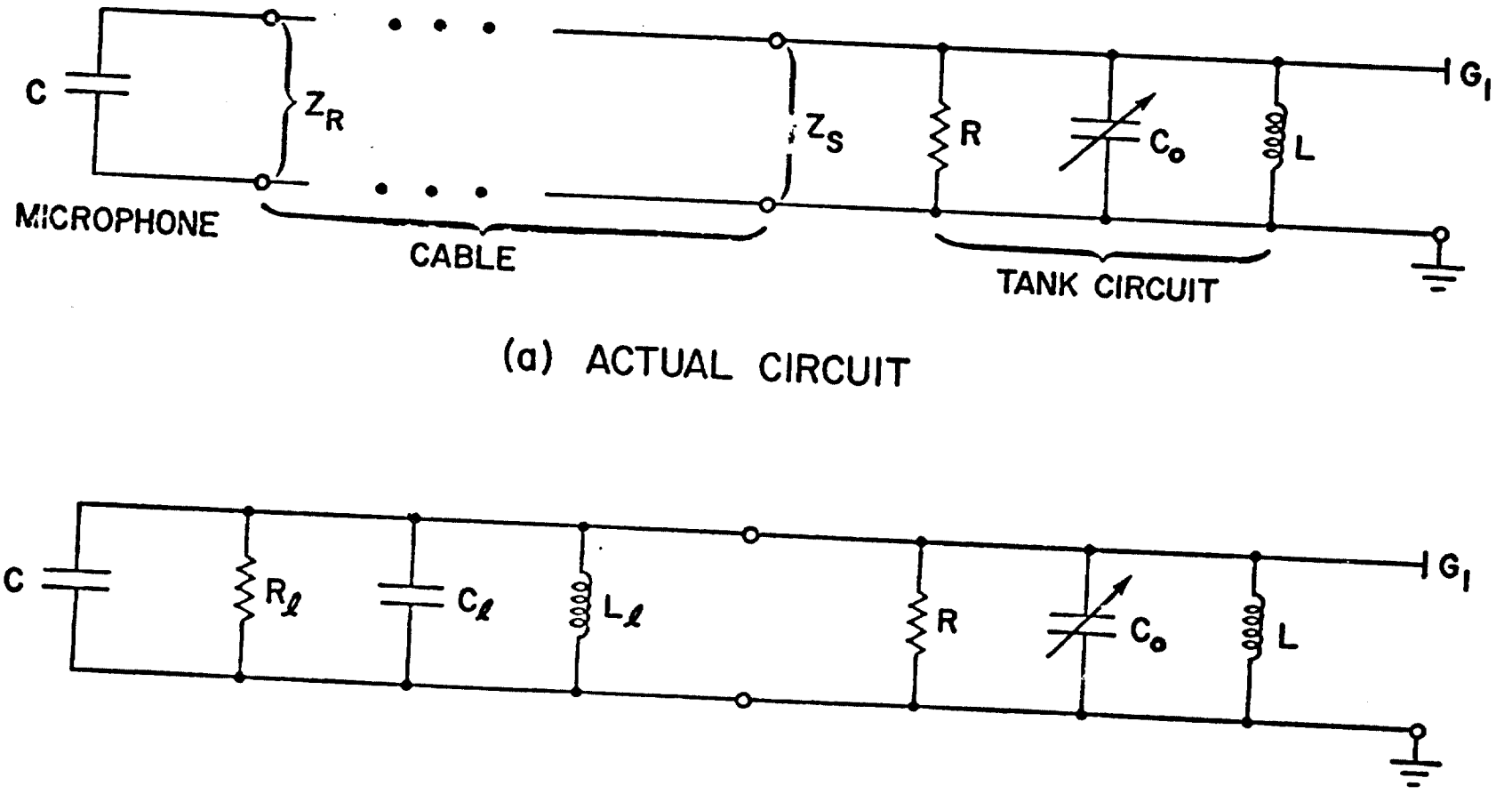

Figure 2. Front end of the converter.

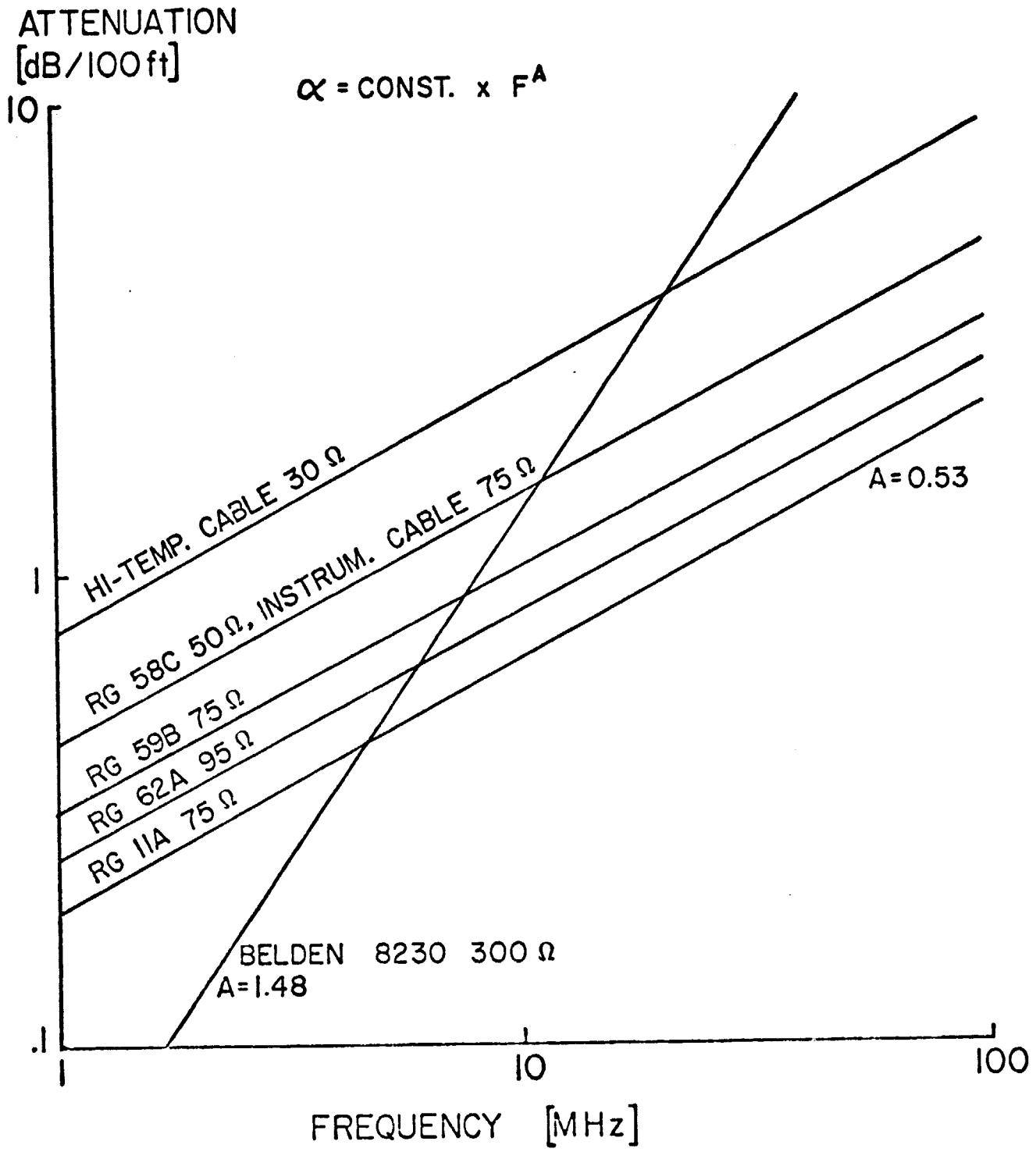

Figure 3. Measured cable attenuation versus frequency.

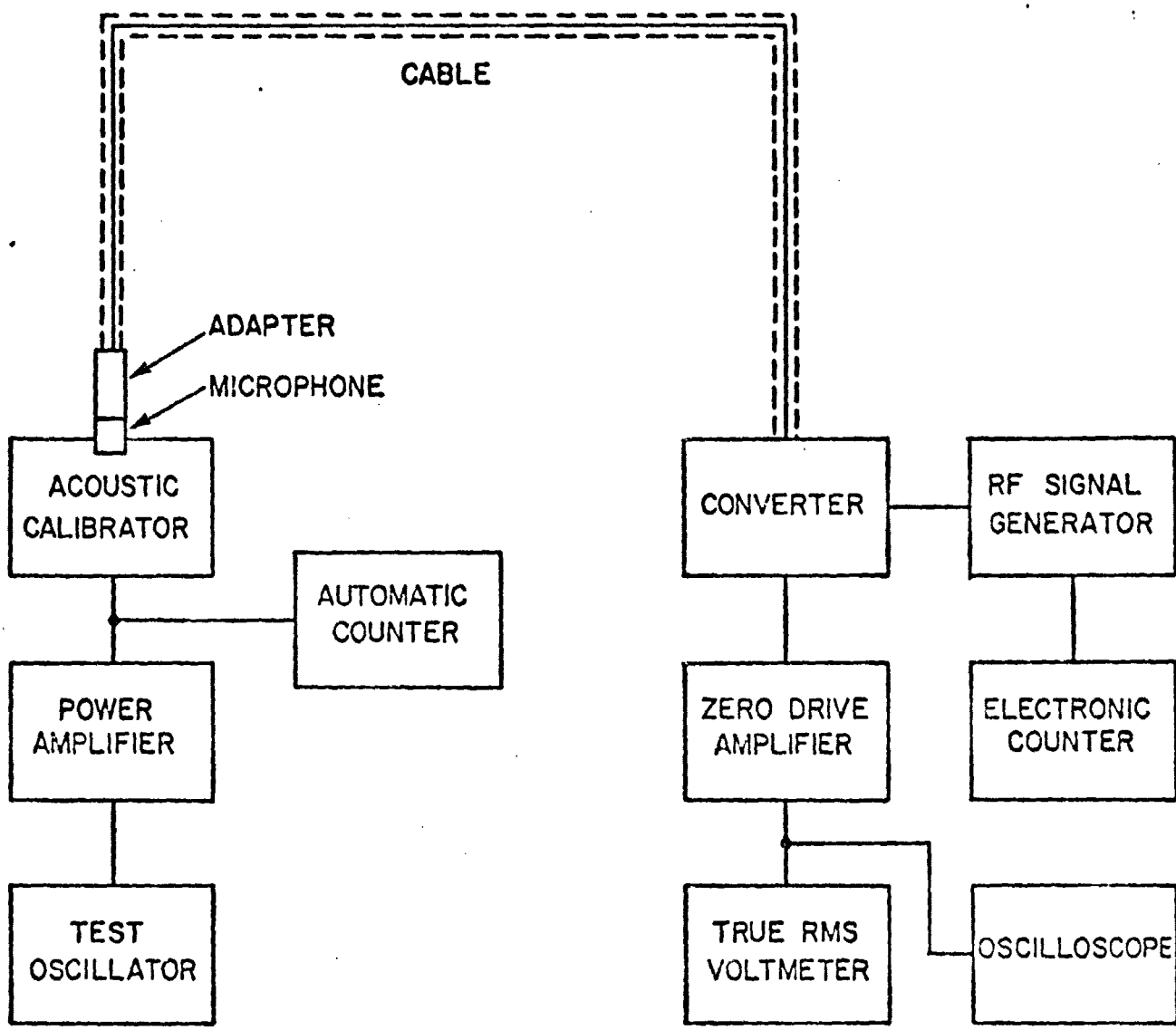

Figure 4. Instrumentation used to measure system sensitivity. Test oscillator = HP651B; power amplifier = HP467A; automatic counter = HP5323A; acoustic calibrator = Whittaker PC-125; microphone = B&K 4134 (SN 469856); converter (see refs. 1 and 2); zero drive amplifier = Gilmore N461 (modified); true rms voltmeter = HP3403C; rf signal generator = HP606B electronic counter = HP5245L; oscilloscope = Tektronix 549 with 1A1 plug-in.

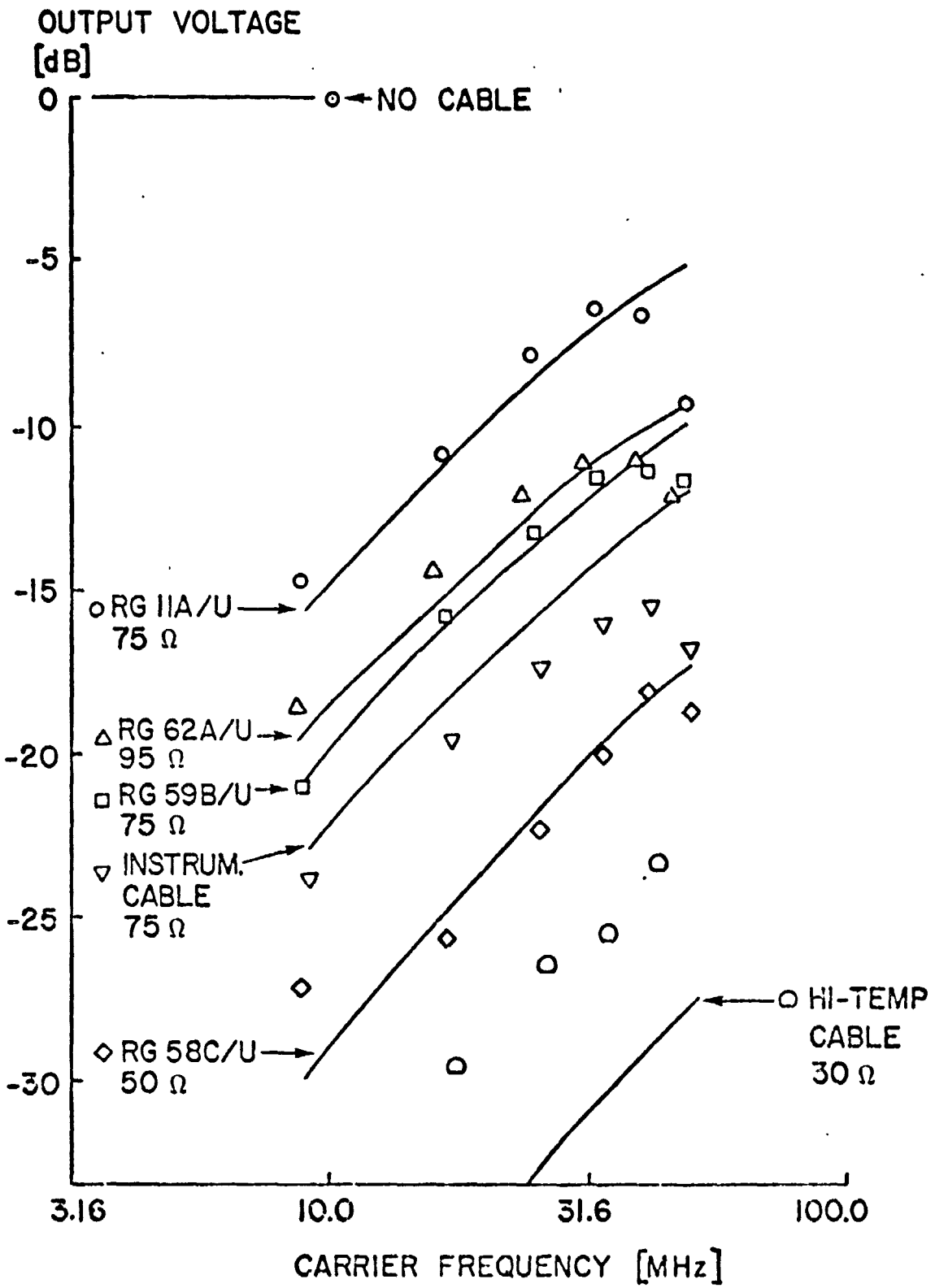

Figure 5. Relative sensitivity of system with various coaxial cables versus carrier frequency.

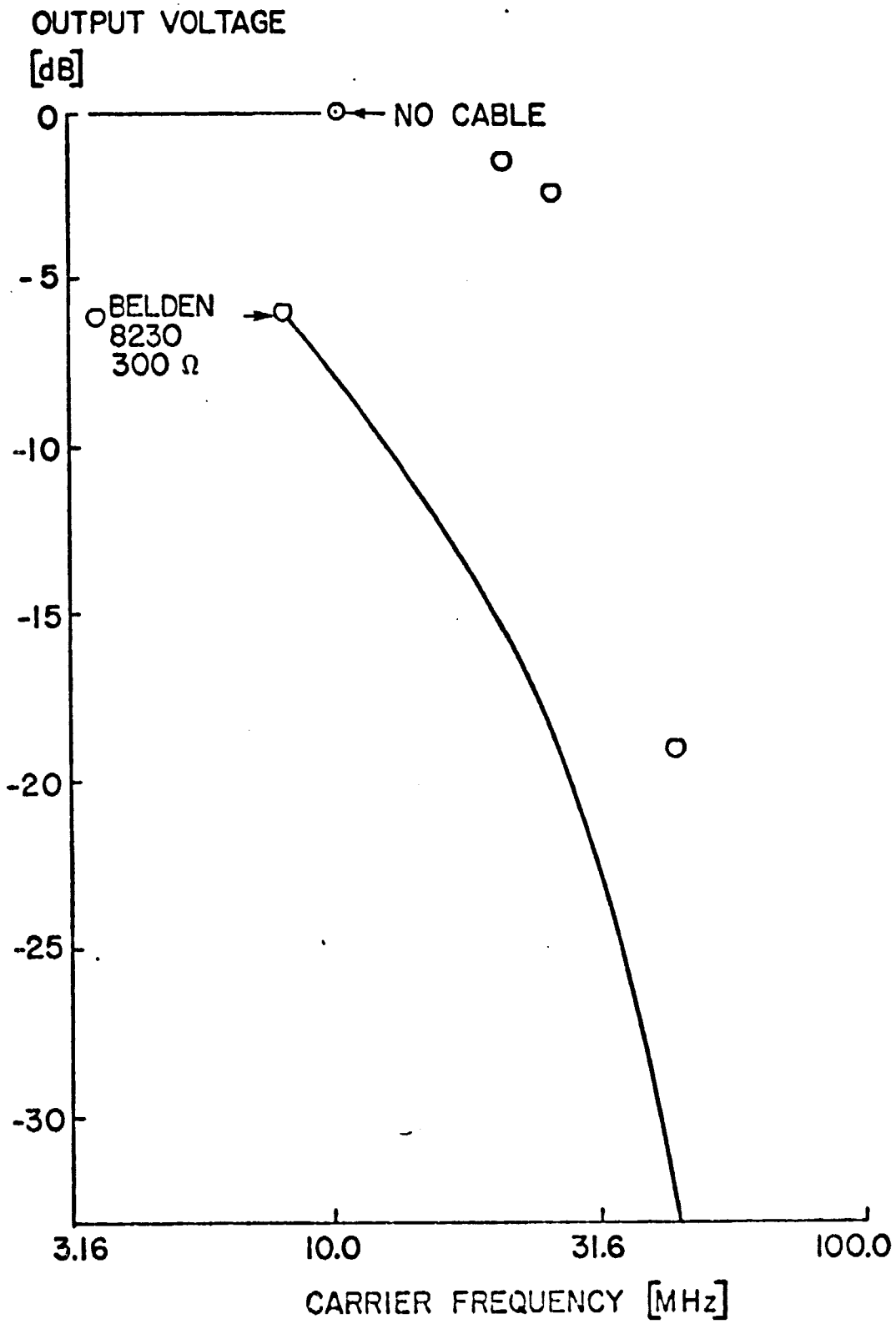

Figure 6. Relative sensitivity of system with parallel-wire cable versus carrier frequency.